Journal of Dentistry 161 (2025) 106007

Contents lists available at ScienceDirect

Journal of Dentistry

journal homepage: www.elsevier.com/locate/jdent

In vitro study of cold atmospheric plasma–induced proliferation inhibition and morphological changes in head and neck carcinoma cell lines

Tatjana Maravic [a], Giulia Petrucci [b], Viviana di Giacomo [b,c], Claudia Mazzitelli [a], Tirtha Raj Acharya [d], Nagendra Kumar Kaushik [d], Eun Ha Choi [d], Monica Rapino [e], Diego D'Urso [a], Uros Josic [a], Vito Carlo Alberto Caponio [f], Massimo Micaroni [g], Mancuso Edoardo [a], Lucio Lo Russo [f], Lorenzo Lo Muzio [f], Lorenzo Breschi [a,*], Vittoria Perrotti [c,h]

[a] University of Bologna (DIBINEM), Dental Clinic, via san Vitale 59, Bologna BO 40125, Italy
[b] Department of Pharmacy, "G. d'Annunzio" University of Chieti-Pescara, Chieti, Via dei vestini, 31, Chieti 66100, Italy
[c] UdA-TechLab, Research Center, "G. d'Annunzio" University of Chieti-Pescara, Via dei vestini, 31, Chieti 66100, Italy
[d] Plasma Bioscience Research Center, Department of Electrical and Biological Physics, Kwangwoon University, 20 Kwangwoon-ro, Nowon-gu, Seoul 01897, South Korea
[e] Genetic Molecular Institute of CNR, Unit of Chieti, "G. d'Annunzio" University of Chieti-Pescara, Via dei Vestini, 31, Chieti 66100, Italy
[f] Department of Clinical and Experimental Medicine, University of Foggia, viale Pinto, 1, Foggia 71122, Italy
[g] Centre for Cellular Imaging Core Facility, Sahlgrenska Academy, University of Gothenburg, Medicinaregatan 5A-7A, Gothenburg 413 90, Sweden
[h] Department of Innovative Technologies in Medicine & Dentistry, University of Chieti-Pescara, Chieti, Italy

ARTICLE INFO

Keywords:
Cold atmospheric plasma
Cell proliferation
Head and neck cancer
Plasma medicine
Electron microscopy

ABSTRACT

Objectives: The use of cold atmospheric plasma (CAP) has been growing in medical field. Since limited data exist on the influence of CAP exposure on head and neck cancer (HNC) cells, we aimed to investigate in vitro its impact on proliferation and morphology of HNC (HSC2, HSC3, and FaDu) cells, as well as healthy gingival fibroblasts (hGF).

Methods: A CAP gas air jet was applied directly on the HSC2, HSC3, FaDu and hGF cells for 30 and 60 s; doxorubicin has been used as positive control. Inhibition of cell proliferation at different time points (24, 48, and 72 h) was investigated through MTS [3-(4,5-dimethylthiazol-2-yl)-5-(3-carboxymethoxyphenyl)-2-(4-sulfophenyl)-2H-tetrazolium]. Morphological alterations were observed using scanning electron microscope (SEM) and transmission electron microscope (TEM). Data were statistically analyzed ($p < 0.05$).

Results: CAP exposure of 60 s showed the highest proliferation inhibitory effects in all investigated cancer cell lines ($p < 0.001$). While HSC2 had the highest proliferation inhibition at 24 h, HSC3, and FaDu exhibited a positive, time-dependent inhibitory effect (24 < 48 < 72 h) after CAP exposure. Interestingly, effects of CAP in the hGF were minimal. SEM observations revealed morphological changes in HNC cells treated with CAP at 30 and 60 s. Moreover, TEM showed stressed conditions in the survived HNC cells at 48 h after CAP exposure demonstrated by the presence of multilamellar and multi-vesicular bodies.

Conclusions: CAP treatment induced proliferation inhibition, morphologic changes and stressed conditions in HNC cell lines (HSC2, HSC3, and FaDu), while demonstrating limited effects on hGF cells.

Clinical Significance: This work characterized early cellular responses of HSC2, HSC3, and FaDu to CAP exposure, including proliferation, and morphology, as foundational data before progressing to more clinically representative models.

* Corresponding author at: Department of Biomedical and Neuromotor Sciences, University of Bologna, Via S. Vitale 59, Bologna (BO), Italia.
E-mail addresses: tatjana.maravic@unibo.it (T. Maravic), giulia.petrucci001@phd.unich.it (G. Petrucci), viviana.digiacomo@unich.it (V. Giacomo), claudia.mazzitelli@unibo.it (C. Mazzitelli), tirtharajacharya@kw.ac.kr (T.R. Acharya), kaushik.nagendra@kw.ac.kr (N.K. Kaushik), ehchoi@kw.ac.kr (E.H. Choi), m.rapino@unich.it (M. Rapino), diego.durso2@unibo.it (D. D'Urso), uros.josic2@unibo.it (U. Josic), vitocarlo.caponio@unifg.it (V.C.A. Caponio), massimo.micaroni@gu.se (M. Micaroni), edoardo.mancuso@unibo.it (M. Edoardo), lucio.lorusso@unifg.it (L.L. Russo), lorenzo.lomuzio@unifg.it (L.L. Muzio), lorenzo.breschi@unibo.it (L. Breschi), v.perrotti@unich.it (V. Perrotti).

https://doi.org/10.1016/j.jdent.2025.106007
Received 16 October 2024; Received in revised form 25 July 2025; Accepted 28 July 2025
Available online 29 July 2025

1. Introduction

Head and neck cancer (HNC) is characterized by poor prognosis (65 % or 40 % 5-year survival if diagnosed in the early or advanced stage, respectively) [1–4]. The traditional therapeutic protocols (surgery, radiotherapy, chemotherapy) are often ineffective and can lead to functional and aesthetic side-effects, dry mouth, rampant onset of dental caries, osteoradionecrosis, etc. [5–7]. These factors have a detrimental effect on the patients' quality of life and recovery [8]. Hence, there is an urgent need of alternative adjuvant therapies [9].

Cold atmospheric plasma (CAP) has emerged in recent years as a promising therapeutical tool in medicine [10,11]. CAP is an ionized gas that has chemical, electromagnetic and thermal effects on the target, due to its ability to react with the surroundings and create radicals, ions and energetic photons [12]. The chemical effects entail the creation of reactive oxygen and nitrogen species (RONS ie. .O, O_2, O_3, .OH, .O_2H, .O_2^-, .O_3^-, .NO, .NO_2) in the gas phase of CAP, and these species seem to be responsible for CAP biological effects, such as regenerative [13,14], anti-inflammatory, antimicrobial, as well as selective cancer cells targeting [4,15,16]. CAP can be directly applied on the substrate (direct application), or indirectly through the administration of CAP-activated liquids (indirect application) [17,18]. However, there is a lack of well-established and standardized protocols before CAP can be approved for clinical use, and further in vitro and in vivo research is warranted [4].

The first step towards the introduction of novel cancer treatments are in vitro studies on cancer cell lines. The 2D in vitro monolayer models remain an essential first step to identify effective exposure conditions, investigate mechanisms of action, and assess differential sensitivity between cancer and normal cells before progressing to more complex 3D or in vivo systems [19]. Different genetic backgrounds and degrees of aggressiveness of NHC cell lines provide a representative panel for evaluating the cellular response to novel anticancer strategies. Recent studies have demonstrated that CAP-treated liquids impaired cell proliferation and induced apoptosis of several HNC cell lines (FaDu, HSC2 and HSC3) [20,21]. Reports in the literature on the effects of a direct plasma exposure on these cells is still lacking up to our knowledge. As to determine the potential side effects of CAP exposure, also healthy cells that could be found in the tissue surrounding the tumor should be investigated. For instance, human gingival fibroblasts (hGF) can be considered as an adequate model for non-tumorigenic oral cells to assess the selectivity of HNC treatment effects. MTS [3-(4,5-dimethylthiazol-2-yl)-5-(3-carboxymethoxyphenyl)-2-(4-sulfophenyl)-2H-tetrazolium] is an assay widely used in oncology research to test the antitumoral effects of novel drugs/therapeutical approaches by assessing cell viability. When cell viability is found reduced, the drugs/therapeutical approaches which are being tested, are considered promising and worthy of further study [22–24].

Hence, the present study aimed to investigate the impact of CAP direct application on HNC cell lines (FaDu, HSC2 and HSC3) and healthy hGF on proliferation inhibition, as well as cell morphology using scanning electron microscopy (SEM) and transmission electron microscopy (TEM).

2. Materials and methods

2.1. Plasma system

An air Jet CAP was employed in the present study. A high-voltage electrode, a ground electrode, a high-voltage power source, and dielectric materials were utilized together with room-temperature air to create cold plasma at atmospheric pressure [25]. A voltage controller was used to control the primary voltage, and the feed air gas flow rate was maintained at a steady 2 liters per minute (lpm). A high voltage electrode made of stainless steel, measuring 1.20 mm by 0.27 mm, served as the inner electrode. Stainless steel was also used to make the ground electrode, which had dimensions of 6 mm in length, 0.27 mm in thickness, and a 0.70 mm centrally drilled hole for plasma formation. A 12 mm distance was kept between the tip of the plasma jet and the target, while a 2 mm discharge gap was maintained between the inner and outer electrodes (Fig. 1a) [26–28].

A digital oscilloscope (WaveSurfer 434; LeCroy, New York, NY, USA), equipped with a high-voltage probe (P6015A; Tektronix, Raleigh, NC, US) and a current probe (CP030; LeCroy, New York, NY, USA), was used for the electrical diagnostics of plasma, including measurements of discharge current, voltage, and the energy and power dissipated in the plasma. The Eqs. (1), (2) and (3) were utilized to calculate the CAP dissipated energy, power and duty cycle [29].

$$\text{Energy (E)} = Q \times V = \int_{t1}^{t2} V(t)I(t)dt \text{ [J]} \quad (1)$$

$$\text{Power (P)} = \text{Duty cycle} \times E \times \frac{1}{t} \text{[W]} \quad (2)$$

The duty cycle can be defined as:

$$\text{Duty cycle (\%)} = \frac{\textbf{On time}}{(\textbf{On time} + \textbf{Off time})} \times 100 \quad (3)$$

where, Q = CAP dissipate charge, V = peak voltage, I = peak current, t = plasma discharge time. Additionally, an optical emission spectrometer (HR4000; Ocean Optics, Orlando, FL, USA) interfaced via an optical fiber was used to study reactive species generated in the plasma. A 400 μm core diameter silica fiber with a numerical aperture (NA) of 0.22 was used to collect the light emitted from the plasma and guide it to the spectrometer. The fiber was placed at an optimized distance of 3 cm away with angle (~ 45 °) from the plasma plume to effectively collect the light while minimizing background interference and signal loss. The species detected were ionized and excited species, radicals, and reactive oxygen and nitrogen species, as detected from the light emitted by the CAP. Fourier transformed infrared spectroscopy (FTIR) in real time was used to determine RONS concentrations in the gas phase with automated FTIR gas analyser (MATRIX-MG5; Bruker, Billerica, MA, US) and a gas analysis software (OPUS GA; Bruker, Billerica, MA, US). A constant flow of CAP system output gas was simultaneously connected to the continuous real-time measurement equipment. Using an ozone monitor (Model 202; B Technologies, Broomfield, CO, US), ozone levels were monitored. The amount of H_2O_2 in 5 mL DW treated with CAP was detected by a peroxide assay kit (QuantiChrom; BioAssay Systems, Hayward, CA, US) which detects peroxides through colorimetric detection using xylenol orange that forms a coloured complex with Fe^{3+} at λ = 585 nm. The quantity of NO^{2-} ions from NO_X (NO, NO_2^- and NO_3^-) was determined by Griss's method for DW after treating it with CAP. A recently published paper provides detailed information on this CAP device and its diagnostics [30]. The plasma temperature in CAP was assessed with a thermal imaging camera (PeakTech P 5620; Meilhaus Electronic, Alling, Germany).

2.2. Cell lines and treatments

Healthy hGF were purchased from Cell Lines Service (Eppelheim, Germany) and cultured in Dulbecco's Modified Eagle's Medium (DMEM/F12; Corning, Manassas, VA, USA) supplemented with heat-inactivated 5 % FBS, 15 mM HEPES, 100 units/mL penicillin, and 100 μg/mL streptomycin (EuroClone, Pero, Italy). FaDu cell line was purchased from American Type Culture Collection (Rockville, MD, USA), and it was grown in Eagle's Minimum Essential Medium (EMEM; Corning, Manassas, VA, USA) supplemented with 1 % Non-Essential Amino Acids (Capricorn Scientific, Ebsdorfergrund, Germany), while HSC2 and HSC3 cell lines were grown in Roswell Park Memorial Institute Medium (Corning, Manassas, VA, USA). All the culture media were

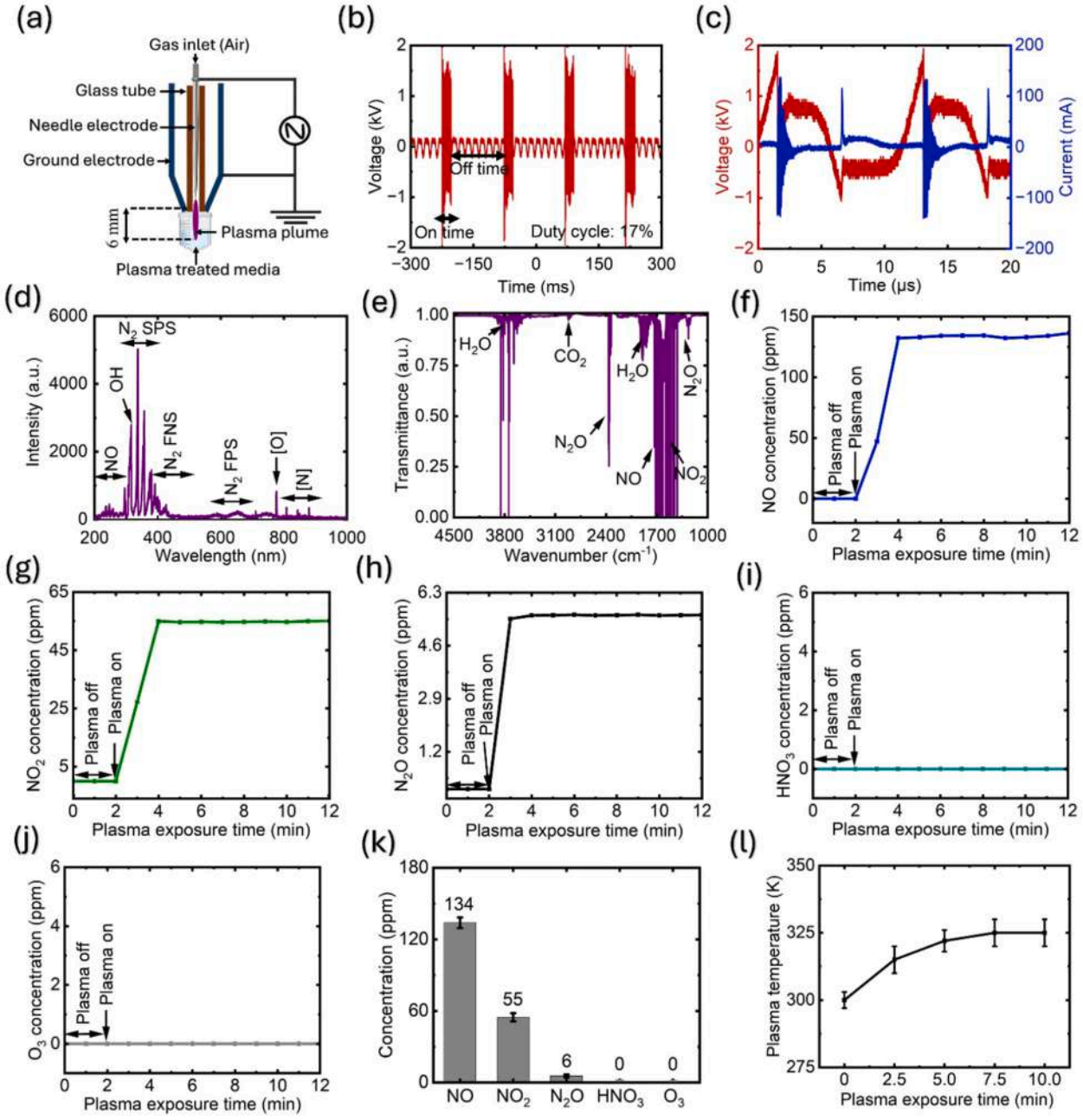

Fig. 1. Cold atmospheric plasma (CAP) setup and diagnostics. (a) CAP configuration, (b-c) duty cycle with current-voltage characterization, (d) optical emission spectroscopy (OES), (e-j) Fourier transform infrared spectroscopy measurement for gas phase reactive species analysis, (k) time average concentration of reactive species generated by CAP within 10 min of plasma exposure, and (l) measurement of plasma temperature with varying plasma exposure time.

supplemented with 10 % heat-inactivated fetal bovine serum (FBS), 100 units/mL penicillin, and 100 μg/mL streptomycin (all from EuroClone, Pero, Italy). All cell lines were maintained at 37 °C in a humidified atmosphere with 5 % CO_2 and maintained in culture for no longer than one month.

The set up of the experiment was performed in cells where the culture media was replaced with fresh media after 24 h of incubation, and CAP direct treatment was applied for 30 s and 60 s; fixed working distance between the capillary of the plasma device and the liquid medium surface containing the cultured cells was set at 12 mm. The parameters were selected based on published literature reporting comparable CAP setups and treatment ranges applied to cancer cell lines [26–28], technical specifications and recommended operating conditions provided by the manufacturer of the CAP device, which indicate ranges commonly used to generate reproducible plasma discharges and the need to apply treatment durations sufficient to induce measurable biological effects, while avoiding excessive thermal damage. Additional experimental point consisted of treating the cells with 1 μM doxorubicin (Doxo; APExBIO, Boston, MA, US) as a positive control for cell death. All experiments involving CAP were conducted in compliance with institutional laboratory safety protocols. Procedures were performed under a certified chemical fume hood with continuous ventilation. Appropriate personal protective equipment (PPE), including lab coats, gloves, and safety goggles, was always to minimize exposure to ozone, hydrogen peroxide, and other reactive plasma-derived species.

2.3. Cell proliferation assay

Cell proliferation was assessed after treatment with MTS (Promega, Madison, WI, USA). Briefly, the day before CAP and Doxo treatments, cells were seeded in 24-well plates at a density of 3×10^4 cells per well in 500 μl of their respective culture medium under standard culture conditions. After 24 h from plating, cells were subjected to treatment with CAP at 30 s and 60 s or with 1 μM Doxo used as positive control of apoptosis. After 24, 48, and 72 h, the MTS solution was directly added to each well at a final concentration of 10 % (v/v) and incubated for 1 h at 37 °C. Cell proliferation was evaluated by measuring the colorimetric absorbance at 490 nm using a multi-plate reader (Spark Multimode; Tecan, Männedorf, Switzerland). Cell proliferation was expressed as percentage of inhibition of cell proliferation after treatments over the cell proliferation inhibition of control cells at 24, 48 and 72 h. Three independent experiments were performed, each carried out in technical triplicate.

2.4. Scanning electron microscopy (SEM) analysis

All the reagents were purchased from Merck (Milan, Italy), unless stated otherwise. Cells were cultured on 12 mm diameter cover glass slides (VWR, Milan, Italy) placed at the bottom of 24-well plates. The cells were subjected to the same treatment described for cell proliferation assay (CAP 30 s, CAP 60 s and Doxo) and then fixed at 24, 48 or 72 h after CAP treatment. Before fixation, the cell medium was removed, and the cells were washed with phosphate-buffered saline (PBS; Euroclone, Pero, Italy). Subsequently, they were fixed in 2.5 % glutaraldehyde in 0.1 M sodium cacodylate buffer (pH = 7.4) and kept at 4 °C for 3 h. After fixation, cells were rinsed three times for 3 min with 0.1 M sodium cacodylate buffer (pH = 7.4). Cells were then post-fixed in osmium tetroxide 1 % in 0.1 M (Electron Microscopy Sciences, Hatfield, PA, US) cacodylate buffer for 30 min, rinsed with 0.1 M sodium cacodylate buffer (pH = 7.4) and dehydrated in ascending concentrations of ethanol (50, 70, 80, 90, 95 and 100 %) and HMDS overnight. Glass slides with dehydrated specimens were mounted on stubs, gold-palladium sputter coated and observed under an SEM (Miraa3; Tescan, Brno, Czech Republic) to investigate cell morphology. Cells that maintained their shape and membrane structure properties were considered unaffected by the CAP exposure. On the other hand, changes in the shape of cells, membrane surface, cell detachment indicated morphological changes.

2.5. Transmission electron microscopy (TEM) analysis and imaging

Cells were cultured on a 35 mm Dish with No 1.5 Coverslip and a 14 mm glass diameter, uncoated (MatTek, Bratislava, Slovak Republic). The cells were subjected to the same treatment with CAP described for the cell proliferation assay but only for 60 s, and the cells were fixed at 48 and 72 h.

All the cell lines were fixed in modified Karnosky's fixative (4 % paraformaldehyde, 1 % glutaraldehyde in 0.1 M cacodylate buffer, all reagents purchased from Merck, Milan, Italy) for 30 min at room temperature, before being moved in diluted fixative 1:10 in cacodylate buffer 0.1 M for 48 h at 4 °C and processed further and embedded in Epoxy resin. Briefly, the samples were then post-fixed with Osmium tetra-Oxide (OsO_4) 1 % (Electron Microscopy Sciences, Hatfield, PA, US) and Potassium Ferrocyanide 1 % in 0.05 M cacodylate buffer at 37 °C for 1 h, and then with Uranyl acetate 1 % (Electron Microscopy Sciences, Hatfield, PA, US) for 30 min at room temperature. The samples were dehydrated stepwise, with increasing concentrations of ethanol, and finally embedded in epoxy resin (Hard-Plus resin; Electron Microscopy Sciences, Hatfield, PA, US) before being polymerized at 60 °C for 16 h.

The embedded specimens were trimmed into a pyramid shape in order to obtain a rectangular surface with a 45° trimming knife (Trim45; Diatome, Nidau, Switzerland) using an ultramicrotome (UC6; Leica, Vienna, Austria). Then, alternate 70 nm thin sections were produced using a 45° diamond knife (Trim45; Diatome, Nidau, Switzerland). The cutting was performed at a cutting speed of 0.8 mm/s.

Imaging was performed at the TEM operating at 120 eKv (Talos L120C; ThermoFisher Scientific, Waltham, MA, US) at a magnification of 2300 × and 11,500 × used with a CMOS, 4 K × 4 K CCD camera (Gatan, Pleasanton, CA, USA). Cells with a good organization and density of mitochondria (m) and Golgi (Ga), lacking the presence of stressed organelles were considered unaffected by the CAP exposure. On the other hand, the presence of phagosomes, multilamellar bodies (MBs) and multi-vesicular bodies (MVB) were indicative of stressing conditions [31].

2.6. Statistical analysis

The data are reported as the representative values of three independent experiments.

To explore the impact of the types of treatment and of the observation times on the percentage of proliferation inhibition, after testing the normality of the data (Shapiro-Wilk), a two-way ANOVA was employed. Bonferroni post-hoc comparison was used to explore differences among subgroups, and an adjusted p-value was set for multiple comparisons significance (0.0166 for the observation times, such as 24, 48 and 72 h; and 0.0125 for the kind of treatment, such as control, Doxo, CAP 30 s and CAP 60 s). All the tests were performed using software (SPSS v25; IBM, Armonk, NY, USA), and the level of significance was set at $p < 0.05$.

3. Results

3.1. CAP plasma diagnostics and RONS analysis

The voltage waveform of CAP was presented in Fig. 1b, which showed a duty cycle of 17 %, an on-time of 24 ms and an off-time of 119 ms. A peak current of 118 mA and a peak voltage of 1.7 kV were recorded by Fig. 1c at the maximum value. The CAP operated at a frequency of 86 kHz, with dissipated energy measured at 0.18 mJ/s and power at 2.6 W [30]. In Fig. 1d, the OES for the CAP cover wavelengths from 200 to 1000 nm. The OES revealed the presence of reactive oxygen and nitrogen species (RONS) such as NOx, OH, nitrogen, and oxygen in the plasma state. Fig. 1e shows the FTIR spectroscopy spectra for the gaseous phase of CAP where the generation of RONS could be detected (4500 – 1000 cm^{-1}). Fig. 1f-j shows the quantification of RONS of CAP in gas phase. The dominant reactive species produced by CAP was NO, followed by NO_2 and N_2O. In contrast, CAP jet cannot produce the HNO_3 and O_3 (Fig. 1i-j). Fig. 1k illustrates the time average concentration of CAP produced with in 10 min of plasma treatment. The main species produced by CAP was NO (134 ppm) and N_2O (55 ppm). Additionally, the time average concentration of N_2O produced by CAP was 6 ppm. Fig. 1l shows the variation in plasma temperature with exposure time from 0 to 10 min. Initially, when there was no plasma, the ambient gas temperature near the nozzle of the reactor was 300 K. On the administration of the CAP treatment for 10 min, this temperature went up to about 325 K. This modest rise is because some portion of the energy input from the plasma discharge is converted into heat, which makes the temperature of the ambient gas near the plasma region increase. Sustained plasma operation and collisions with ambient air molecules further contribute to this localized heat effect [32].

To analyse the CAP generated RONS in liquid phase, the levels of H_2O_2 and NO_2^- in DW during the first 10 min of CAP treatment. Initially, both concentrations were zero. After 10 min of treatment, H_2O_2 reached 40.2 μM and NO_2^- reached 1380 μM. The increase in these concentrations is due to the reactive species produced in the plasma. Specifically, NO reacts with oxygen and water vapor to form H_2O_2, and it reacts with water to produce NO_2^- in the plasma, air, and liquid phases [33].

3.2. CAP direct application exerted an inhibition of HNC cells proliferation

Cell proliferation inhibition of three HNC cell lines (HSC2, HSC3, and FaDu), as well as of normal hGF cells was measured at different time points 24, 48, and 72 h as presented on Fig. 2.

Two-way ANOVA model did not detect a statistically significant interaction between the treatments and the observation times for the hGF ($p = 0.568$). CAP 30 s did not impact the cell viability, while CAP 60 s reported a statistically significant increase of proliferation inhibition compared to both the control ($p < 0.001$) and CAP 30 s ($p < 0.001$). Among different observation times (24, 48, 72 h), no statistically significant difference emerged, regardless of the different treatments.

For the HSC2 cell line, two-way ANOVA detected a statistically significant interaction between treatment group and observation time ($p < 0.001$). The effect of both CAP 30 s and CAP 60 s, decreased progressively from 24 to 72 h. The highest inhibitory effect was observed for CAP 60 s with significant differences with control and CAP 30 s ($p < 0.001$).

Similarly, for HSC3 cell line, two-way ANOVA detected a statistically significant interaction between treatment group and observation time ($p < 0.001$). The effect of both CAP 30 s and CAP 60 s, increased progressively from 24 to 72 h. While for the HSC2 cell line the highest effect in cell proliferation inhibition was observed at 24 h, for HSC3 cell line this was seen at 72 h. Again, the CAP 60 s treatment resulted as the most effective in decreasing cell proliferation with significant differences with both control and CAP 30 s ($p < 0.001$).

FaDu cell line behavior resulted very similar to HSC3 cell line ($p < 0.001$).

3.3. SEM analysis of the morphology of CAP-treated cell lines

Representative SEM images of each investigated cell line are presented on Figs. 3–6 in ascending magnifications. In the control group, flattened, stretched, cells were observed, indicative of the normal fibroblast morphology. The cell density of hGF was not affected by CAP direct application, while the morphology was largely preserved in the CAP 30 s group, with slight rounding of the normally spindle-shaped cells in the CAP 60 s group (Fig. 3). On the contrary, rounding and blebbing of the cell membrane were noted in the Doxo group. In the HNC cell lines, rounded and cobblestone shaped in the control group, the density of the cells was significantly affected both by CAP treatment and Doxo. The morphology of all the cancer cell lines was greatly affected by Doxo treatment, with blebs, destruction of the cell membrane, and cell shrinking. While CAP 30 s led to minor changes in cell morphology of HSC3 (cell shrinking) and FaDu cell lines (Figs. 5 and 6, respectively), cell damage with flattening of the cells was evident in the HSC2 cells (Fig. 4). The CAP 60 s treatment demonstrated a more evident influence on cell morphology than CAP 30 s, with cell detachment and modifications of the cell membrane.

3.4. Ultrastructure of CAP-treated cell lines using TEM

The exposure of the cell lines to the plasma for 60 s was monitored after 48 h using TEM. Here the status of the survived cells was investigated, and their intracellular ultrastructure is shown in Fig. 7. Similar morphological results were found after 72 h CAP exposure (data not shown).

HGFs were used as control being a non-cancer cell line. Looking at their status 48 h after the plasma exposure, no significant stressed organelles were observed, nor the presence of phagosomes. In addition, hGFs showed an overall organization of Ga and m comparable to the pre-exposure cells. The overall number of cells was similar as in the control group.

On the other hand, the plasma exposure caused a drastic decrease of HSC2 and HSC3 cells; the few survived cells after 48 h of exposure showed an increased intracellular amount of MBs (empty arrowheads) MVBs (full arrowheads), all indicative of stressing conditions. Furthermore, in the HSC3 the accumulation of these organelles was visually higher than in the HSC2, and the mitochondria were losing most of their normal structure, in terms of cristae organization as well as shape and size.

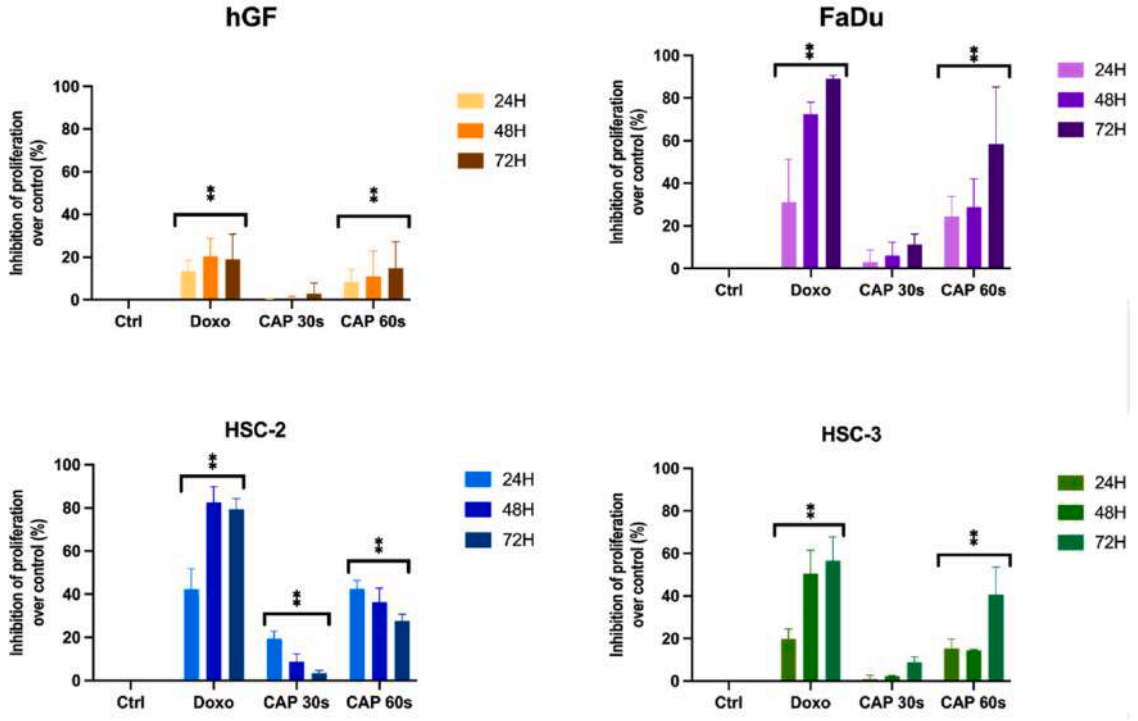

Fig. 2. Graphical representation of the inhibition of proliferation compared to the control (%) of the different investigated cell lines at 24, 48 and 72 h after treatment. Asterisks mark groups significantly different from each other and from control ($p < 0.05$).

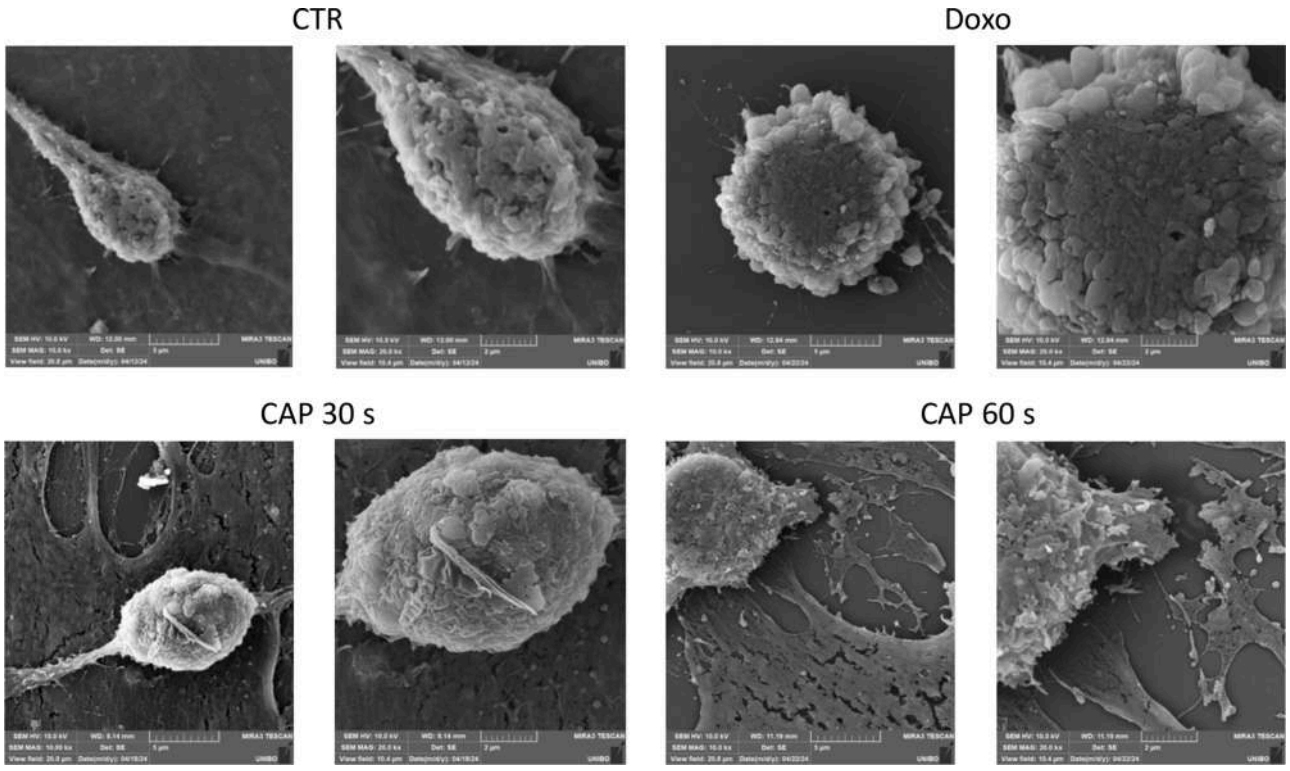

Fig. 3. Representative scanning electron microscopy images of the hGF cell line with different treatments. Magnifications, 10.000 × (left image) and 20.000 × (right image). CTR – control group; Doxo – doxorubicin; CAP – cold atmospheric plasma.

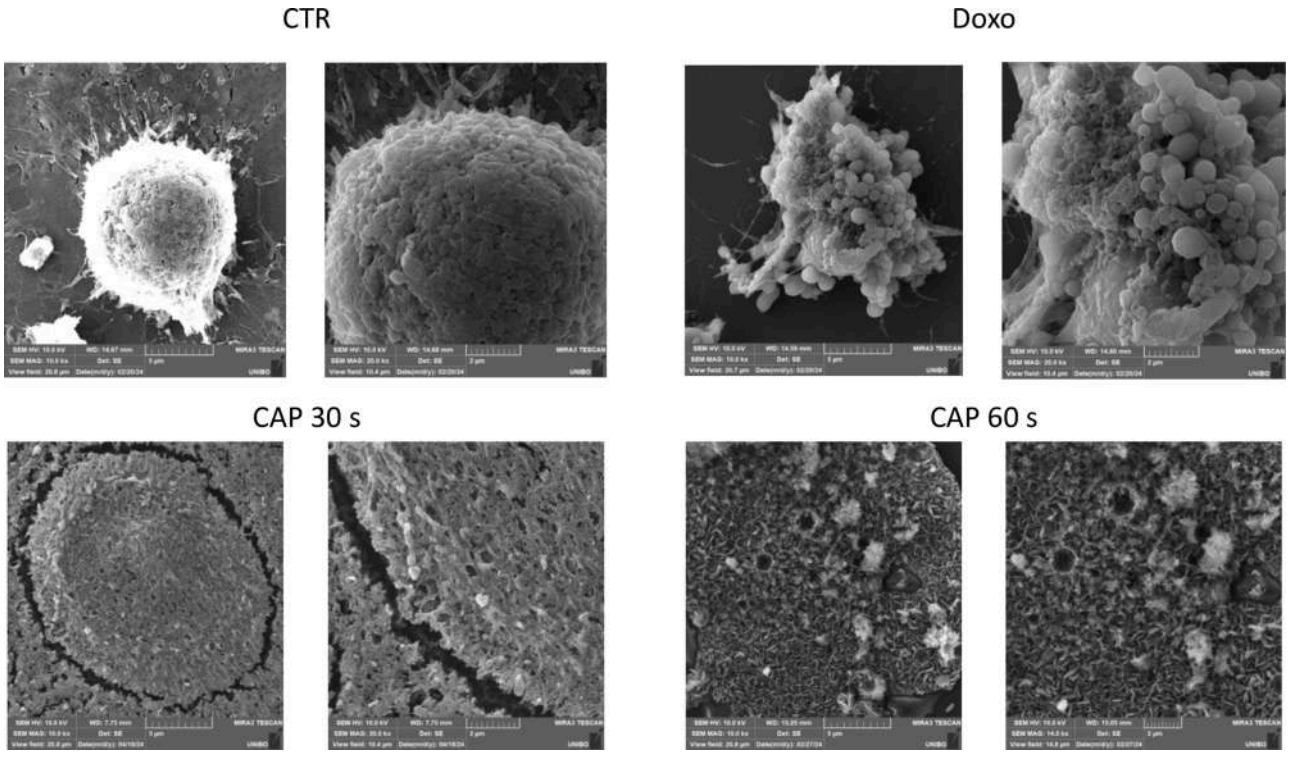

Fig. 4. Representative scanning electron microscopy images of the HSC2 cell line with different treatments. Magnifications, 10.000 × (left image) and 20.000 × (right image). CTR – control group; Doxo – doxorubicin; CAP – cold atmospheric plasma.

In the FaDu cell line, the stressful conditions were less evident compared to the other two cancer cell lines. The only presence of MVBs was coupled with substantial overall good organization and density of mitochondria.

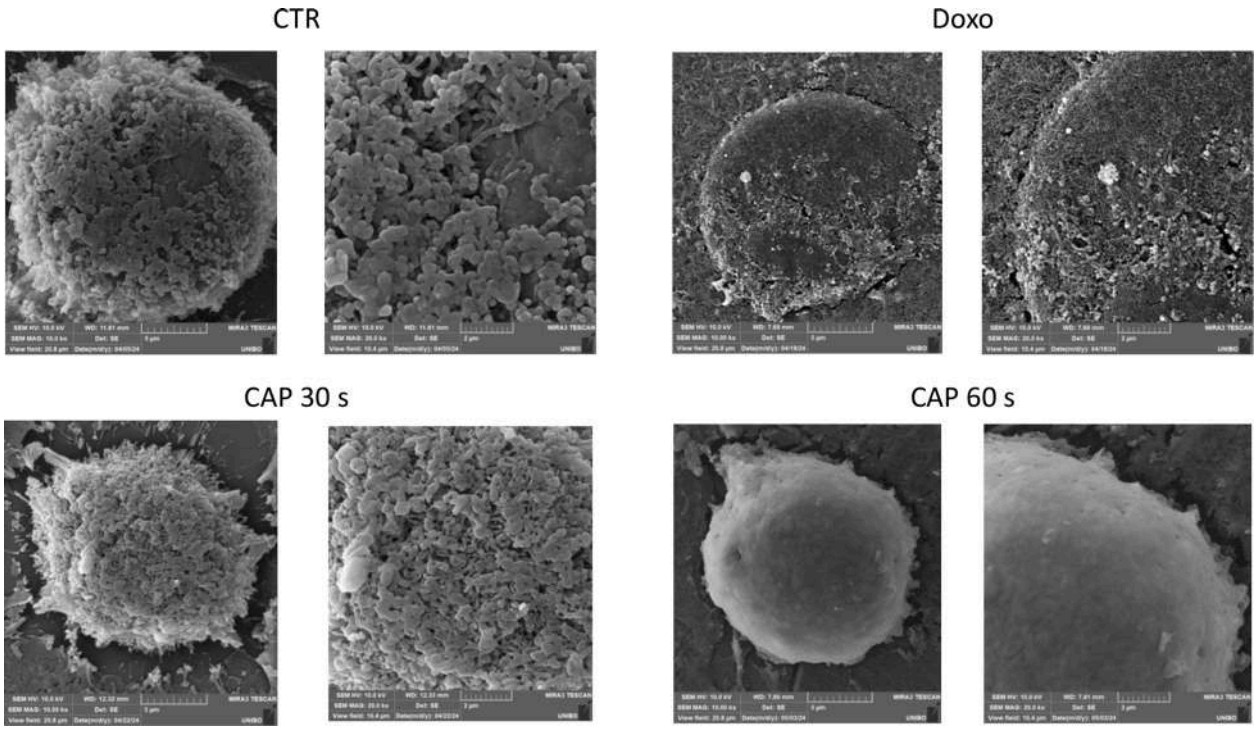

Fig. 5. Representative scanning electron microscopy images of the HSC3 cell line with different treatments. Magnifications, 10.000 × (left image) and 20.000 × (right image). CTR – control group; Doxo – doxorubicin; CAP – cold atmospheric plasma.

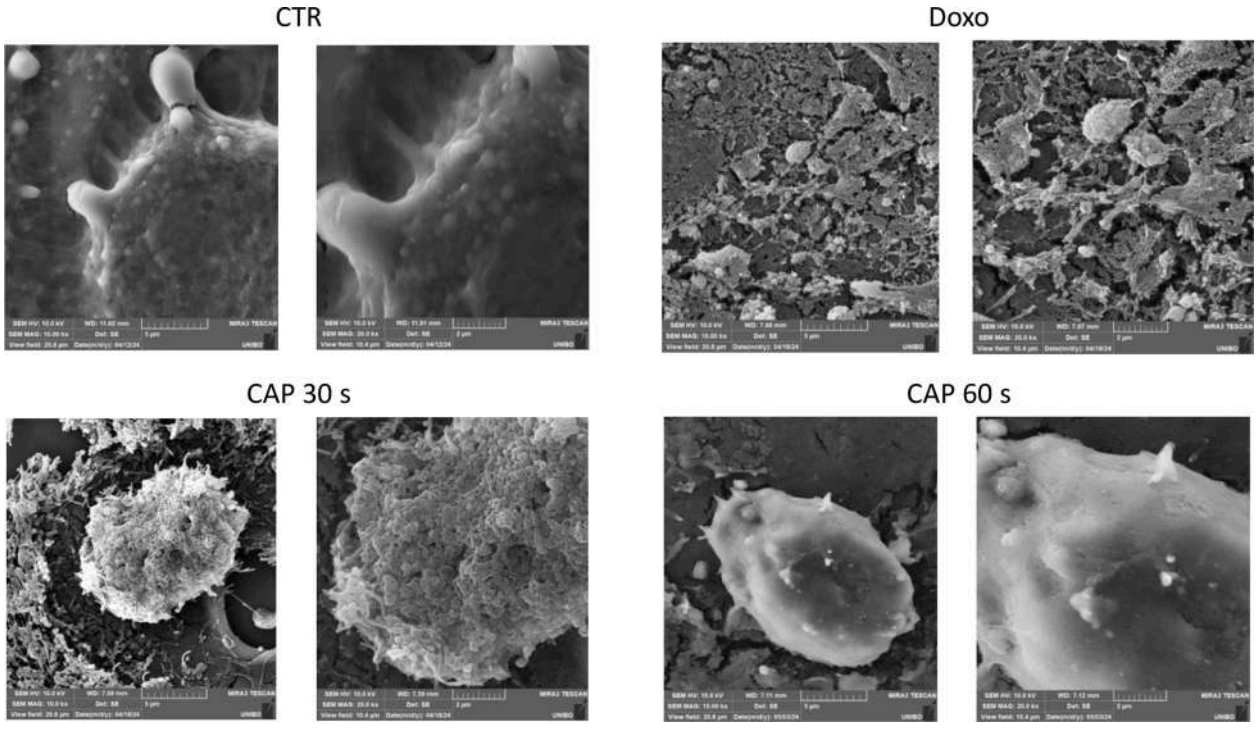

Fig. 6. Representative scanning electron microscopy images of the FaDu cell line with different treatments. Magnifications, 10.000 × (left image) and 20.000 × (right image). CTR – control group; Doxo – doxorubicin; CAP – cold atmospheric plasma.

4. Discussion

The present study investigated the effect of CAP direct for 30 s or 60 s on the inhibition of the proliferation of HNC cell lines (FaDu, HSC2 and HSC3) and of hGF. Direct exposure to CAP significantly impacted the HNC cell lines investigated in the present study by inhibiting cell proliferation and altering their morphology. This process generates RONS, such as NO_X, H_2O_2, and OH, that were shown to lead to cell cycle arrest and cell death [34]. CAP was previously demonstrated to alter the structural integrity of human hepatocellular carcinoma cells, causing morphological changes such as cell shrinkage, membrane blebbing, and loss of adhesion [35]. Furthermore, inhibition of proliferation and

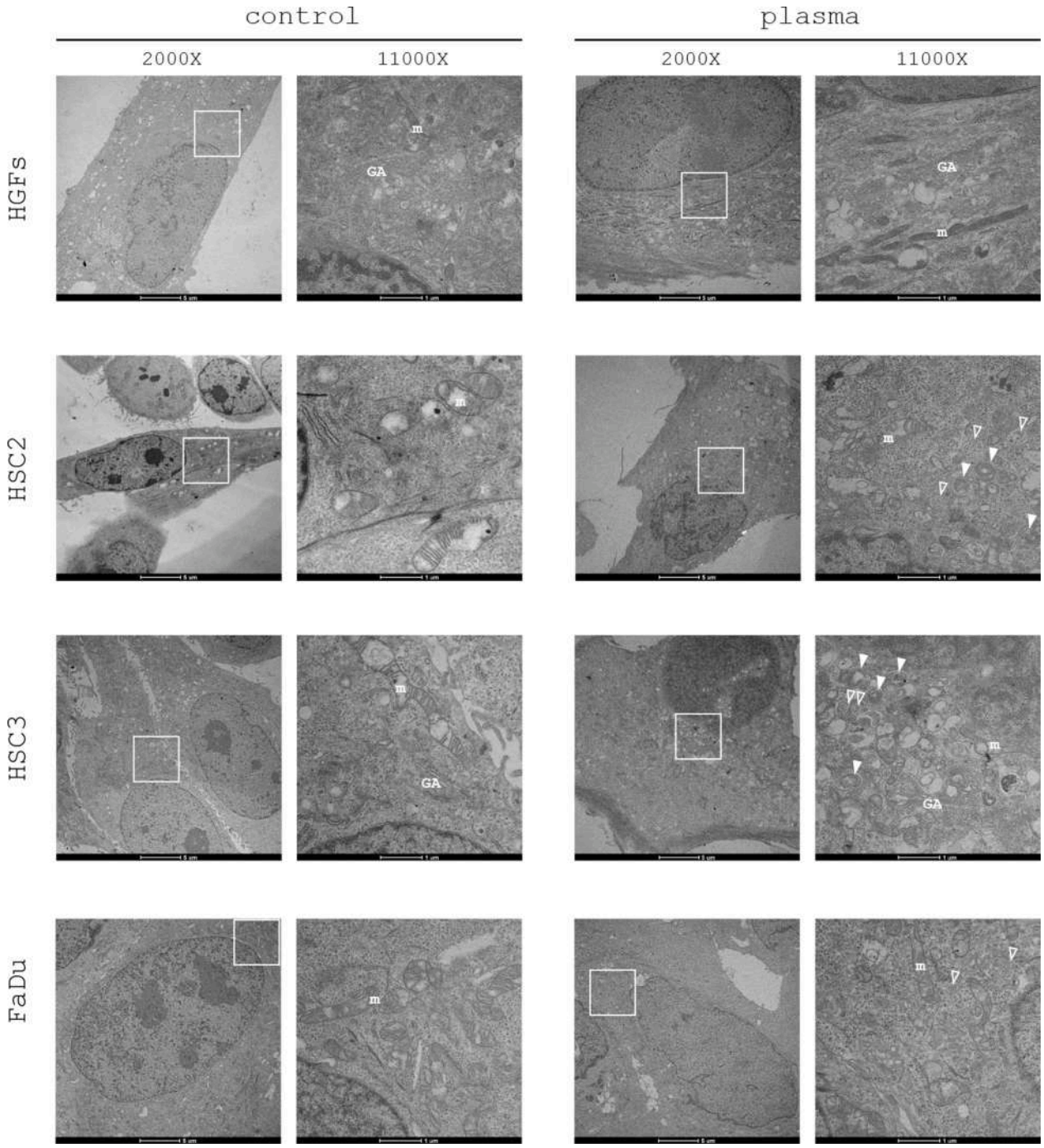

Fig. 7. Representative transmission electron microscopy images of HGF, HSC2, HSC3 and FaDu cell lines with different treatments. Magnifications 2000 × (first and third columns) and 11,000 × (second and fourth columns). The white insets in the lower magnification pictures are the area represented in the higher magnification pictures.
GA: Golgi Apparatus; m: mitochondria; Empty arrowheads: multi-vesicular bodies (MVBs) and full arrowheads: multilamellar bodies (MBs).

apoptosis occurrence of FaDu, HSC2 and HSC3 cell lines exposed to CAP-activated media (indirect CAP treatment) were previously reported [20,21]. Our results on direct CAP exposure are in line with the previous findings, since CAP exposure increased FaDu, HSC2 and HSC3 proliferation inhibition. Further, CAP impaired their morphology in a time-dependent manner. The effects of CAP, however, were much more pronounced in the investigated cancer cell lines compared to the healthy control (hGF), demonstrating the potential non-toxicity of CAP to healthy cells. These effects collectively hinder the proliferation of HNC FaDu, HSC2 and HSC3 cells under controlled in vitro conditions, indicating that the direct interaction between plasma-generated reactive species and HNC cancer cell lines can be considered for testing in more clinically representative models, such as 3D tumor spheroids, or ex vivo tissues. Cell lines such as FaDu, HSC2 and HSC3 are well-established and widely used in vitro models for studying HNC squamous cell carcinoma [20,21], while the use of hGFs in the present study is justified by their anatomical and physiological relevance to the oral environment, as they are resident stromal cells in close proximity to the tumor microenvironment in vivo.

The more pronounced effects of CAP on FaDu, HSC2 and HSC3

cancer cells is probably due to the chemical effects of CAP. Namely, the RONS produced by CAP treatment induce intracellular oxidative stress and endoplasmic reticulum stress. Given that cancer cells have a higher basal level of ROS, it is more likely that the levels will surpass the cellular limit, leading to DNA and mitochondrial damage and consequently, apoptosis [36]. The endoplasmic reticulum stress increases the intracellular calcium ions concentration and precipitates protein CHOP, leading to depolarization of the mitochondrial membrane [37]. A recent study revealed that CAP induces HNC cell (SAS cell line) death through other pathways, such as autophagy, ferroptosis by diminishing oncogenic miRNA expression and survival signals [38,39]. Further, CAP physical properties, such as heat, ultraviolet irradiation and electromagnetic field possibly contributed to the specificity of the CAP treatment towards FaDu, HSC2 and HSC3 cells. Moreover, CAP treatment can influence the interaction between the immune system and tumor microenvironment []. By causing immunogenic cancer cells death, it could trigger the immune response of the organism against the investigated cancer cell lines [40]. CAP was also shown to reduce tumor angiogenesis and tumor stroma desmoplasia [39]. Another underlying mechanism of CAP cancer cell targeting could be the disfunction in the epidermal growth factor receptor, which is overexpressed in the oral squamous cell carcinoma, caused by the nitric oxide radicals [41].

Our results supported the selectivity of CAP treatment towards the investigated HNC cell lines compared to healthy hGF, which is in accordance with several other studies in the literature, demonstrating both non-apoptotic [42] and apoptotic [41,43] cell death pathways. The effects of CAP revealed in the present study were dose-dependent (CAP 60 s generally induced more proliferation inhibition) and observation time-dependent (24 < 48 < 72 h). While CAP 30 s did not influence hGF viability, a certain percentage of proliferation inhibition was noted with CAP 60 s treatment. Hence, in a future vision of a potential clinical use after testing on clinically relevant models, care should be taken to apply a dose of CAP that would induce oxidative cellular stress high enough to exceed the cellular limit in cancer cells, but not in healthy cells. These findings were corroborated by the TEM analysis results, which demonstrated a preservation of the organization of Ga and mitochondria in the hGF, while MVs and MLVs were present in the FaDu, HSC2 and HSC3 cell lines. Multi-lamellar bodies form in the process of active autophagy [44]. Further, although all investigated cancer cell lines were impacted by CAP treatment, there were certain variabilities among the cell lines. While HSC3 and FaDu cell lines demonstrated a similar trend of time-dependent increase of proliferation inhibition, HSC2 cell line demonstrated the highest CAP effects at 24 h. Also, the FaDu cell line seemed to have less signs of stress in the TEM analysis compared to other cancer cell lines. This could possibly be due to cell mutations or different phases in the cell cycle. For instance, disruptive TP53 mutations can cause resistance to radiotherapy; thus, one may hypothesize that this mutation could also influence CAP treatment efficiency. Also, cells in the S phase of the cell cycle might be more susceptible to CAP [42].

Similarly to the TEM analysis, the morphological SEM analysis supported the proliferation inhibition results. CAP exposure influenced FaDu, HSC2 and HSC3 cell morphology with a dose-dependent trend. CAP 60 s application caused more evident modifications of the cell membrane morphology, while CAP 30 s exposure caused cell shrinking and changes in the morphology. Doxo treatment demonstrated evident influence in all the tested cell lines, with blebs on the membrane and cell shrinking. Only few other studies [43,45] investigated HNC cell lines morphology using electron microscopy, and our findings are in line with the findings of those research groups.

The present in vitro study contributes to the pool of research on influence of CAP application on HNC cells, and the specific setup parameters can be replicated and validated in other studies. The limitation of the present work is the fact that it is an exploratory mechanistic in vitro study on monolayer cell model, and not a clinically simulated exposure protocol. Future research will focus on integrating physical barriers and more advanced models to approximate clinical relevance and refine dosage calibration. However, it was important to firstly establish an initial assessment of the direct interaction between plasma-generated reactive species and HNC cell lines, under controlled in vitro conditions, as well as characterize early cellular and molecular responses, including proliferation, and morphology, as foundational data before progressing to more clinically representative models.

5. Conclusions

CAP exposure for 30 and 60 s inhibited the proliferation of certain HNC cell lines in vitro. Furthermore, CAP exposure altered the morphology of the cells and brought them in a stressed state, with the presence of MBs and MVBs. The effects of CAP were found to be less prominent in the healthy hGF cell line.

Data availability

Data is available obtained and analyzed in the current study are available from the corresponding author upon a reasonable request.

Fundings

This study was financed by the European Union - NextGenerationEU through the Italian Ministry of University and Research under PNRR 2022 “Therapeutical effects of Cold atmospheric plasma in Head And Neck Cancer and oral hEalth preservation - C.H.A.N.C.E.?”, cod: 2022ATYY5B settore LS7. Giulia Petrucci has been funded with a scholarship within the PhD programme in Medical Biotechnologies at the University of Chieti, Cycle XXXIXbis, financed by the Ministerial Decree no 118 of 2nd March 2023, based on the NRRP - funded by the European Union - NextGenerationEU - Mission 4 "Education and Research", Component 1 "Enhancement of the offer of educational services: from nurseries to universities” - Investment 4.1 “Extension of the number of research doctorates and innovative doctorates for public administration and cultural heritage”- CUP D53C23002170003

CRediT authorship contribution statement

Tatjana Maravic: Writing – original draft, Investigation, Formal analysis, Data curation. **Giulia Petrucci:** Writing – original draft, Investigation, Data curation. **Viviana di Giacomo:** Writing – review & editing, Validation, Methodology, Investigation. **Claudia Mazzitelli:** Writing – review & editing, Project administration, Data curation. **Tirtha Raj Acharya:** Writing – review & editing, Resources, Methodology. **Nagendra Kumar Kaushik:** Writing – review & editing, Resources, Methodology. **Eun Ha Choi:** Writing – review & editing, Validation, Resources. **Monica Rapino:** Writing – review & editing, Investigation. **Diego D’Urso:** Writing – review & editing, Investigation. **Uros Josic:** Writing – original draft, Visualization, Investigation. **Vito Carlo Alberto Caponio:** Writing – original draft, Formal analysis, Data curation. **Massimo Micaroni:** Writing – original draft, Investigation, Formal analysis. **Mancuso Edoardo:** Writing – original draft, Visualization, Software. **Lucio Lo Russo:** Writing – review & editing, Supervision, Funding acquisition. **Lorenzo Lo Muzio:** Writing – review & editing, Conceptualization. **Lorenzo Breschi:** Writing – review & editing, Supervision, Project administration, Funding acquisition, Conceptualization. **Vittoria Perrotti:** Writing – review & editing, Supervision, Funding acquisition, Conceptualization.

Declaration of competing interest

The authors declare no competing interests.

Acknowledgements

We acknowledge the Centre for Cellular Imaging (CCI) at University

of Gothenburg and the National Microscopy Infrastructure, NMI (VR-RFI 2019-00217) for providing assistance in microscopy. We thank also COST Actions CA20114 (Therapeutical Applications of Cold Plasmas) for the stimulating environment provided. We would also like to thank Prof. Gabriella Teti and Dr. Valentina Papa (University of Bologna) for providing trainig and support for the preparation of cells for microscopy observation.

References

[1] M.F. Svahn, C. Munk, T.S.S. Nielsen, C. von Buchwald, K. Frederiksen, S.K. Kjaer, Trends in all-cause five-year mortality after head and neck cancers diagnosed over a period of 33 years. Focus on estimated degree of association with human papillomavirus, Acta Oncol. (Madr) 55 (2016) 1084–1090, https://doi.org/10.1080/0284186X.2016.1185148.

[2] National Cancer Institute, Cancer Stat Facts: Oral Cavity and Pharynx Cancer, https://Seer.Cancer.Gov/Statfacts/Html/Oralcav.Html (n.d.).

[3] L.Q.M. Chow, Head and neck cancer, New Eng. J. Med. 382 (2020) 60–72, https://doi.org/10.1056/NEJMra1715715.

[4] V. Perrotti, V.C.A. Caponio, L.Lo Muzio, E.H. Choi, M.C. Di Marcantonio, M. Mazzone, N.K. Kaushik, G. Mincione, Open questions in cold atmospheric plasma treatment in head and neck cancer: a systematic review, Int. J. Mol. Sci. 23 (2022), https://doi.org/10.3390/ijms231810238.

[5] I. Brook, Late side effects of radiation treatment for head and neck cancer, Radiat. Oncol. J. 38 (2020) 84–92, https://doi.org/10.3857/roj.2020.00213.

[6] A.S. Pierik, C.R. Leemans, R.H. Brakenhoff, Resection margins in head and neck cancer surgery: an update of residual disease and field cancerization, Cancers (Basel) 13 (2021) 2635, https://doi.org/10.3390/cancers13112635.

[7] S.R. Cunha, T. Maravic, A. Comba, P.A. Ramos, F.R. Tay, D.H. Pashley, E. Rodrigues, A. Cecília, A. Mazzoni, L. Breschi, In vivo and in vitro radiotherapy increased dentin enzymatic activity, J. Dent. 100 (2020) 103429, https://doi.org/10.1016/j.jdent.2020.103429.

[8] C.Zecena Morales, K. Lisy, L. McDowell, A. Piper, M. Jefford, Return to work in head and neck cancer survivors: a systematic review, J. Cancer Surviv. 17 (2023) 468–483, https://doi.org/10.1007/s11764-022-01298-6.

[9] R. Elaldi, L.-M. Roussel, J. Gal, B. Scheller, E. Chamorey, R. Schiappa, A. Lasne-Cardon, M.-Y. Louis, D. Culié, O. Dassonville, G. Poissonnet, E. Saada, K. Benezery, E. Babin, A. Bozec, Correlations between long-term quality of life and patient needs and concerns following head and neck cancer treatment and the impact of psychological distress. A multicentric cross-sectional study, Eur. Arch. Otorhinolaryngol. 278 (2021) 2437–2445, https://doi.org/10.1007/s00405-020-06326-8.

[10] S.B. Borkar, M. Negi, A. Jaiswal, T. Raj Acharya, N. Kaushik, E.H. Choi, N. K. Kaushik, Plasma-generated nitric oxide water: a promising strategy to combat bacterial dormancy (VBNC state) in environmental contaminant micrococcus luteus, J. Hazard. Mater. 461 (2024) 132634, https://doi.org/10.1016/j.jhazmat.2023.132634.

[11] P. Patel, N. Kaushik, T.R. Acharya, E.H. Choi, N.K. Kaushik, Surface air gas discharge plasma: an ecofriendly virus inactivation approach to enhance CPRRs mediated antiviral genes expression against airborne bio-contaminant (human Coronavirus-229E), Environ. Pollut. 347 (2024) 123700, https://doi.org/10.1016/j.envpol.2024.123700.

[12] A. Bogaerts, E.C. Neyts, Plasma technology: an emerging technology for energy storage, ACS Energy Lett. 3 (2018) 1013–1027, https://doi.org/10.1021/acsenergylett.8b00184.

[13] W.L. Hui, V. Perrotti, F. Iaculli, A. Piattelli, A. Quaranta, The emerging role of cold atmospheric plasma in implantology: a review of the literature, Nanomaterials 10 (2020) 1505, https://doi.org/10.3390/nano10081505.

[14] W.L. Hui, D. Ipe, V. Perrotti, A. Piattelli, Z. Fang, K. Ostrikov, A. Quaranta, Novel technique using cold atmospheric plasma coupled with air-polishing for the treatment of titanium discs grown with biofilm: an in-vitro study, Dent. Mater. 37 (2021) 359–369, https://doi.org/10.1016/j.dental.2020.11.027.

[15] O. Assadian, K.J. Ousey, G. Daeschlein, A. Kramer, C. Parker, J. Tanner, D. J. Leaper, Effects and safety of atmospheric low-temperature plasma on bacterial reduction in chronic wounds and wound size reduction: a systematic review and meta-analysis, Int. Wound J. 16 (2019) 103–111, https://doi.org/10.1111/iwj.12999.

[16] M. Vandamme, E. Robert, S. Lerondel, V. Sarron, D. Ries, S. Dozias, J. Sobilo, D. Gosset, C. Kieda, B. Legrain, J. Pouvesle, A.Le Pape, ROS implication in a new antitumor strategy based on non-thermal plasma, Int. J. Cancer 130 (2012) 2185–2194, https://doi.org/10.1002/ijc.26252.

[17] S.B. Borkar, M. Negi, T.R. Acharya, P. Lamichhane, N. Kaushik, E.H. Choi, N. K. Kaushik, Mitigation of T3SS-mediated virulence in waterborne pathogenic bacteria by multi-electrode cylindrical-DBD plasma-generated nitric oxide water, Chemosphere 350 (2024) 140997, https://doi.org/10.1016/j.chemosphere.2023.140997.

[18] P. Lamichhane, T.R. Acharya, N. Kaushik, L.N. Nguyen, J.S. Lim, V. Hessel, N. K. Kaushik, E.H. Choi, Non-thermal argon plasma jets of various lengths for selective reactive oxygen and nitrogen species production, J. Environ. Chem. Eng. 10 (2022) 107782, https://doi.org/10.1016/j.jece.2022.107782.

[19] M.A. Tutty, S. Holmes, A. Prina-Mello, Cancer cell culture: the basics and two-dimensional cultures, Methods Mol. Biol. 2645 (2023) 3–40, https://doi.org/10.1007/978-1-0716-3056-3_1.

[20] V. di Giacomo, M. Balaha, A. Pece, I. Cela, G. Fulgenzi, G. Orsini, T. Spadoni, T. R. Acharya, N.K. Kaushik, E.H. Choi, M. Rapino, M. Mazzone, G. Mincione, G. Sala, E. Sardella, V. Perrotti, Human head and neck cancer cell lines response to cold atmospheric plasma activated media is affected by the chemistry of culture media, Heliyon 11 (2025) e41458, https://doi.org/10.1016/J.HELIYON.2024.E41458.

[21] V. di Giacomo, M. Balaha, M. Pinti, M.C. Di Marcantonio, I. Cela, T.R. Acharya, N. K. Kaushik, E.H. Choi, G. Mincione, G. Sala, M. Perrucci, M. Locatelli, V. Perrotti, Cold atmospheric plasma activated media selectively affects human head and neck cancer cell lines, Oral Dis. 31 (2025) 401–416, https://doi.org/10.1111/ODI.15120.

[22] B. Wang, A.Y. Xing, G.X. Li, L. Liu, C. Xing, SNHG14 promotes triple-negative breast cancer cell proliferation, invasion, and chemoresistance by regulating the ERK/MAPK signaling pathway, IUBMB Life 76 (2024) 1295–1308, https://doi.org/10.1002/IUB.2910.

[23] J.J. Qu, X.Y. Qu, D.Z. Zhou, miR-4262 inhibits colon cancer cell proliferation via targeting of GALNT4, Mol. Med. Rep. 16 (2017) 3731–3736, https://doi.org/10.3892/MMR.2017.7057/HTML.

[24] S. Sae-Lim, B. Soontornworajit, P. Rotkrua, Inhibition of colorectal cancer cell proliferation by regulating platelet-derived growth factor B signaling with a DNA aptamer, Asian Pac. J. Cancer Prev. 20 (2019) 487, https://doi.org/10.31557/APJCP.2019.20.2.487.

[25] T.R. Acharya, P. Lamichhane, A. Jaiswal, K. Amsalu, Y.J. Hong, N. Kaushik, N. K. Kaushik, E.H. Choi, The potential of multicylindrical dielectric barrier discharge plasma for diesel-contaminated soil remediation and biocompatibility assessment, Environ. Res. 240 (2024) 117398, https://doi.org/10.1016/j.envres.2023.117398.

[26] N.K. Kaushik, N. Kaushik, M. Adhikari, B. Ghimire, N.N. Linh, Y.K. Mishra, S.J. Lee, E.H. Choi, Preventing the solid cancer progression via release of anticancer-cytokines in co-culture with cold plasma-stimulated macrophages, Cancers (Basel) 11 (2019) 842, https://doi.org/10.3390/CANCERS11060842.

[27] N.K. Kaushik, N. Kaushik, R. Wahab, P. Bhartiya, N.N. Linh, F. Khan, A.A. Al-Khedhairy, E.H. Choi, Cold atmospheric plasma and gold quantum dots exert dual cytotoxicity mediated by the cell receptor-activated apoptotic pathway in glioblastoma cells, Cancers (Basel) 12 (2020) 457, https://doi.org/10.3390/CANCERS12020457.

[28] P. Bhartiya, K. Masur, D. Shome, N. Kaushik, L.N. Nguyen, N.K. Kaushik, E.H. Choi, Influence of redox stress on crosstalk between fibroblasts and keratinocytes, Biology (Basel) 10 (2021) 1338, https://doi.org/10.3390/BIOLOGY10121338/S1.

[29] T.R. Acharya, P. Lamichhane, A. Jaiswal, N. Kaushik, N.K. Kaushik, E.H. Choi, Evaluation of degradation efficacy and toxicity mitigation for 4-nitrophenol using argon and air-mixed argon plasma jets, Chemosphere 358 (2024) 142211, https://doi.org/10.1016/j.chemosphere.2024.142211.

[30] V. Puca, B. Marinacci, M. Pinti, F. Di Cintio, B. Sinjari, M.C. Di Marcantonio, G. Mincione, T.R. Acharya, N.K. Kaushik, E.H. Choi, M. Sallese, S. Guarnieri, R. Grande, V. Perrotti, Antimicrobial efficacy of direct air gas soft jet plasma for the in vitro reduction of oral bacterial biofilms, Sci. Rep. 14 (2024) 10882, https://doi.org/10.1038/s41598-024-61438-z.

[31] P.H. Raven, G. Johnson, K.A. Mason, J. Losos, S. Singer, Biology, 11th ed., McGraw Hill, New York, 2016.

[32] Y. Miao, A. Yokochi, G. Jovanovic, S. Zhang, A. von Jouanne, Application-oriented non-thermal plasma in chemical reaction engineering: a review, Green Energy Resour. 1 (2023) 100004, https://doi.org/10.1016/j.gerr.2023.100004.

[33] P. Lukes, B.R. Locke, J. Brisset, Aqueous-phase chemistry of electrical discharge plasma in water and in gas–liquid environments. Plasma Chemistry and Catalysis in Gases and Liquids, Wiley, Hoboken, 2012, pp. 243–308, https://doi.org/10.1002/9783527649525.ch7.

[34] D. Hua, D. Cai, M. Ning, L. Yu, Z. Zhang, P. Han, X. Dai, Cold atmospheric plasma selectively induces G_0/G_1 cell cycle arrest and apoptosis in AR-independent prostate cancer cells, J. Cancer 12 (2021) 5977–5986, https://doi.org/10.7150/jca.54528.

[35] Y. Wang, X. Mang, D. Li, Y. Chen, Z. Cai, F. Tan, Piezoeletric cold atmospheric plasma induces apoptosis and autophagy in human hepatocellular carcinoma cells through blocking glycolysis and AKT/mTOR/HIF-1α pathway, Free Radic. Biol. Med. 208 (2023) 134–152, https://doi.org/10.1016/j.freeradbiomed.2023.07.036.

[36] Z. Zou, H. Chang, H. Li, S. Wang, Induction of reactive oxygen species: an emerging approach for cancer therapy, Apoptosis 22 (2017) 1321–1335, https://doi.org/10.1007/s10495-017-1424-9.

[37] R. Moniruzzaman, M.U. Rehman, Q.L. Zhao, P. Jawaid, Y. Mitsuhashi, S. Imaue, K. Fujiwara, R. Ogawa, K. Tomihara, J. ichi Saitoh, K. Noguchi, T. Kondo, M. Noguchi, Roles of intracellular and extracellular ROS formation in apoptosis induced by cold atmospheric helium plasma and X-irradiation in the presence of sulfasalazine, Free Radic. Biol. Med. 129 (2018) 537–547, https://doi.org/10.1016/j.freeradbiomed.2018.10.434.

[38] Y.C. Cheng, K.W. Chang, J.H. Pan, C.Y. Chen, C.H. Chou, H.F. Tu, W.C. Li, S.C. Lin, Cold atmospheric plasma jet irradiation decreases the survival and the expression of oncogenic miRNAs of oral carcinoma cells, Int. J. Mol. Sci. 24 (2023), https://doi.org/10.3390/ijms242316662.

[39] S. Förster, Y. Niu, B. Eggers, M. Nokhbehsaim, F.J. Kramer, S. Bekeschus, A. Mustea, M.B. Stope, Modulation of the tumor-associated immuno-environment by non-invasive physical plasma, Cancers (Basel) (2023) 15, https://doi.org/10.3390/cancers15041073.

[40] N.D. Almeida, A.L. Klein, E.A. Hogan, S.J. Terhaar, J. Kedda, P. Uppal, K. Sack, M. Keidar, J.H. Sherman, Cold atmospheric plasma as an adjunct to immunotherapy for glioblastoma multiforme, World Neurosurg. 130 (2019) 369–376, https://doi.org/10.1016/j.wneu.2019.06.209.

[41] J.H. Lee, J.Y. Om, Y.H. Kim, K.M. Kim, E.H. Choi, K.N. Kim, Selective killing effects of cold atmospheric pressure plasma with no induced dysfunction of epidermal growth factor receptor in oral squamous cell carcinoma, PLoS One 11 (2016), https://doi.org/10.1371/journal.pone.0150279.

[42] R. Guerrero-Preston, T. Ogawa, M. Uemura, G. Shumulinsky, B.L. Valle, F. Pirini, R. Ravi, D. Sidransky, M. Keidar, B. Trink, Cold atmospheric plasma treatment selectively targets head and neck squamous cell carcinoma cells, Int. J. Mol. Med. 34 (2014) 941–946, https://doi.org/10.3892/ijmm.2014.1849.

[43] C. Oh, H.R. Won, W.S. Kang, D.W. Kim, S.N. Jung, M.A. Im, L. Liu, Y.L. Jin, Y. Piao, H.J. Kim, Y.E. Kang, M.J. Lee, J.Y. Heo, S. Jun, N.S. Sim, J.H. Lee, K. Song, Y. Il Kim, J.W. Chang, B.S. Koo, Head and neck cancer cell death due to mitochondrial damage induced by reactive oxygen species from nonthermal plasma-activated media: based on transcriptomic analysis, Oxid. Med. Cell. Longev. 2021 (2021) 9951712, https://doi.org/10.1155/2021/9951712.

[44] M. Hariri, G. Millane, M.-P. Guimond, G. Guay, J.W. Dennis, I.R. Nabi, Biogenesis of multilamellar bodies via autophagy, Mol. Biol. Cell 11 (2000) 255–268.

[45] B.B. Choi, Y.S. Choi, H.J. Lee, J.K. Lee, U.K. Kim, G.C. Kim, Nonthermal plasma-mediated cancer cell death; targeted cancer treatment, J. Therm. Sci. Technol. 7 (2012) 399–404, https://doi.org/10.1299/jtst.7.399.